Comparative Analysis of Performance Between Artificial Neural Networks and Support Vector Machines on Satellite Image Classification using Landsat data in Yola, Nigeria

Auwal Aliyu
ZASTAL, Kano.
National Space Research and Development Agency.
Abuja, Nigeria.
Email: auwalaliyu508@gmail.com

Muhammad Isma'il
Department of Geography and Environmental Management. Ahmadu Bello University.
Zaria, Nigeria.
Email: migeogjameel@gmail.com

Sule Muhammad Zubairu
Department of Geography and Environmental Management. Ahmadu Bello University.
Zaria, Nigeria
Email: sulemuhd@gmail.com

***Abstract*- Image classification is being used these days to bridge the vision gap between computers and humans so that machines can identify images in the same way that humans do. Its focus is on assigning the appropriate class to the given image. In recent years, there has been an increasing overlap between the data science and remote sensing fields due to free satellite data, high-end consumer computer power, and user-friendly programming tools. There are several remote sensing applications that have made use of data from the USGS missions specifically. Nevertheless, there are few research that use this data to assess how well machine learning and deep learning algorithms work in the complex Yola North environment. The purpose of this research is to evaluate the classification performance of two types of machine learning and deep learning algorithms: support vector machines (SVM) and artificial neural networks (ANN). Using Landsat 8 images of 2022 covering the Yola-North Local Government Area in northern Nigeria, the study analyses a mixed-use environment with four land use and land cover classifications (such as built-up, vegetation, water, and bare soil). Metrics obtained from an error matrix were utilized to evaluate the accuracy, however, the Kappa coefficient and the overall accuracy were the main factors considered while distributing the algorithm hierarchy. Based on the results, support vector machines generated the highest overall accuracy (95.5%).**

Keywords- Machine Learning, Support Vector Machine, Deep Learning, Artificial Neural Network, Satellite image, Classification, Classifier.

I. INTRODUCTION

Image classification is a tool used by computer vision in research, work, and daily activities. For land-use change analysis, the Land Use Land Cover (LULC) classification process is crucial [1]. Image preprocessing, segmentation, key feature extraction, and training site selection are all steps in LULC classification. However, improving LULC classification requires selecting an optimal algorithm due to the ground covering complexity [2]. To identify the optimum classifier for the characteristics of the study, an assessment of different classification methods is needed, because a good result depends on the model setup, sample size, and characteristics of an area [3]. Remote sensing applications have made good use of several well-established and conventional classification techniques, including maximum likelihood and minimum distance, in addition to deep learning and machine learning techniques. Remarkable advancements in image classification have been made possible by the advent of machine learning and deep learning classification techniques, particularly Support Vector Machine (SVM) and Artificial Neural Networks (ANN), respectively, as well as the availability of high-resolution remote sensing data [4].

Support Vector Machine is a sort of machine learning classification approach, that optimizes the distance between the support vectors of each class by building a hyperplane between each class hence decreasing classification inaccuracies [5]. It is a supervised learning classification method that allows for obtaining accurate classifications from a set of small training samples [6]. Artificial Neural Network, On the other hand, is a deep learning classifier, which simulates human neural synapses. It is a supervised learning Model that uses the processing of the brain as a basis to create an algorithm that can be utilized for classification and prediction [7].

Numerous comparative researches have been carried out to evaluate the effectiveness of different machine learning classifiers. In a comparison of Random forests, Extreme gradient boosting, and Deep Learning, SVM was able to obtain a comparatively high overall accuracy of 0.758 in a land cover classification in the landscape of South-central Sweden, that involves eight land-cover classes [9]. Recently, [10] examined the effects of training sample size on the accuracy of crop type mapping in central Morocco using SVM ANN and Maximum Likelihood (ML). They found that SVM achieved overall accuracies of 85.83%, 81.12%, and 89% respectively, using optical, Radar, and Optical combined with SAR. [11] evaluated SVM and compared it to ANN for the purpose of classifying land cover on US volcanic islands located in the Aleutian Arc. They discovered that SVM achieved the best classification accuracy (98.08%). [12] discovered that, in a flat area in the south of Hungary, the Support Vector Machine proved to be the most effective algorithm, surpassing both RF and ANN in the classification of land use and land cover using Sentinel 2B Level 2A images in temporarily waterlogged areas. However,

in a comparison of Decision Tree (DT), SVM, and ANN for Land Cover Classification Using Sentinel-2A Data in the city of Soran, Kurdistan region, Iraq [13] reported a higher accuracy of ANN (90%) as compared to SVM (65%) and DT (60%). Whereas, a land-cover classification with spectral angle mapper (SAM), Mahalanobis Distance (MD) Random Forest (RF), Support Vector Machine (SVM), Artificial Neural Network (ANN), and Fuzzy Adaptive Resonance Theory-supervised predictive Mapping (Fuzzy ARTMAP), in river Ganga, India, published by [14], resulted in higher accuracy of RF (0.89). Furthermore, a parametric Maximum Likelihood (ML) method was tested for per-pixel image classification on satellite observations [15] [16]. However, LULC classification faces challenges due to inadequate sampling as well as spectral and spatial limitations due to atmospheric and illumination effects [17] [18]. It is obvious from the above studies, that attention has not been given to comparing the accuracy of Machine Learning and Deep Learning classifiers for LULC classification in the complex Yola North landscape which has implications on the quality, and integrity of outputs of the classification results. It is against this background that this research evaluates the performance of Machine Learning (SVM) and Deep Learning (ANN) classifiers in modeling the LULC of Yola-North LGA, Adamawa State, Nigeria.

A. Motivation and objectives

Classification using satellite images provides an essential foundation for tracking LULC changes as it helps determine the extent of LULC features. [1]. For this study, satellite data from the Land Sat series was chosen because of its excellent spatial detail of 15 meters and 30 meters resolution and the fact that its radiometric measurement spans eleven (11) separate bands in the visible, Microwave, thermal, and infrared. Studies are currently utilizing these data to assess the effectiveness of emerging Deep Learning, and Machine Learning classifiers for classification in some parts of the world. The goal of this research is to assess the classification efficacy of ANN and SVM algorithms, employing land Sat data over the Yola-North landscape in Adamawa state, Nigeria.

B. Algorithms Selection

SVM was selected based on its inherent robustness to multi-dimensional data sets like satellite images and provides a distinct segmentation of the predefined classes, thereby avoiding confusion and obtaining precise classifications from a lower number of training samples [5]. Likewise, It was demonstrated that ANNs could function well even with complicated, partial, or erroneous input data [13] [14] [7]. The Machine Learning and Deep Learning algorithms, that are compared are the ones that are often utilized in the field of remote sensing (SVM) and data science (ANN), both of which are gaining popularity in remote sensing [9] [19].

II. THE STUDY AREA

The study area lies between longitudes 12° 19' 12" and 12° 30' 0" east of the Greenwich Meridian and latitudes 9° 12' 0." and 9° 21' 0" north of the equator. Situated on the Benue River's bank, the region is bordered to the north and east by Giere and to the south and west by the Yola-South local government area. The city has an estimated area of approximately112.74Km². Fig. 1 shows the location of the study area: Yola-North.

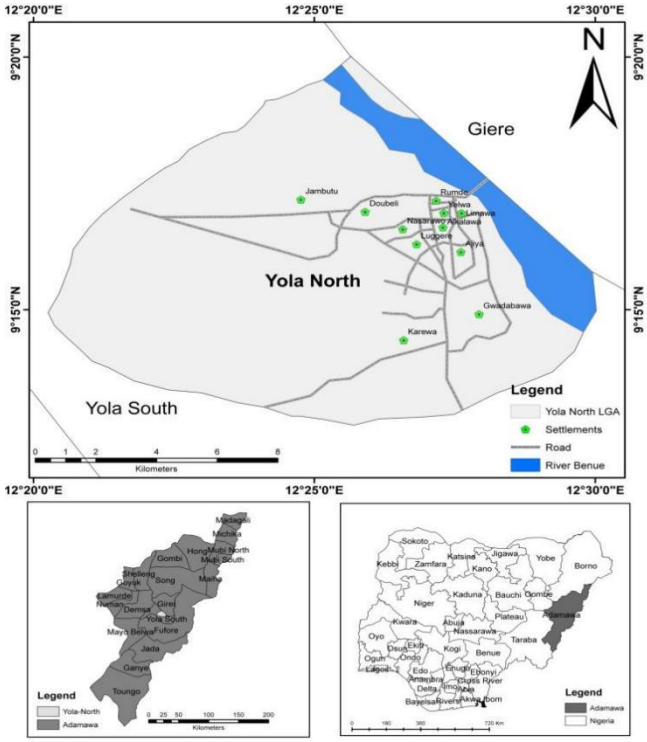

Fig. 1. Location of the Study Area: Yola-North LGA

III. DATA

Data from Land sat 8 satellites that observe the Earth at 30m, 15m, and 100m spatial resolutions were utilized to create the multispectral image. The highest spatial resolution among publicly accessible satellite products is 15 m. The inclusion of three visible (Red, Green, and Blue) and Near Infrared (NIR) bands, that are able to record the intense reflectance of vegetation in the near-infrared portion of the electromagnetic spectrum (EMS) and built-up, water, and bare surface in RGB, is another feature of the land sat data. The criteria for the selection of satellite images required that the scenes have low to no haze or clouds. The image used was a February 16, 2022, Land Sat 8 OLI image (Fig. 2). TABLE 1 demonstrates that the band architectures of the Land Sat satellites are not identical, and the range of the mean center wave-length of the four spectral bands considered in this research is between 0.45 and 0.90 micrometers (mm). The satellite images were obtained from the USGS Open access portal at: earthexplorer.usgs.gov. Furthermore, for accuracy assessment of the classification results, a sample size of two hundred ground truth points (that is, fifty ground truth points for every land use Land cover category) was obtained from the field using a Global Positioning System (GPS) device based on stratified random sampling [20]

TABLE 1: BAND ARCHITECTURE OF LANDSAT 8 IMAGE

Land Sat 8 Spectral Bands	Wavelength (mm)	Resolution (m)
Band1-Coastal aerosol	0.43-0.45	30
Band 2-Blue	0.45-0.51	30
Band 3-Green	0.53-0.59	30
Band 4-Red	0.64-0.67	30
Band 5-NIR	0.85-0.88	30
Band 6-SWIR 1	1.57-1.65	30
Band 7-SWIR 2	2.11-2.29	30
Band 8-Panchromatic	0.50-0.68	15
Band 9-Cirrus	1.36-1.38	30
Band 10-TIRS 1	10.6-11.19	100
Band 11-TIRS 2	11.50-12.51	100

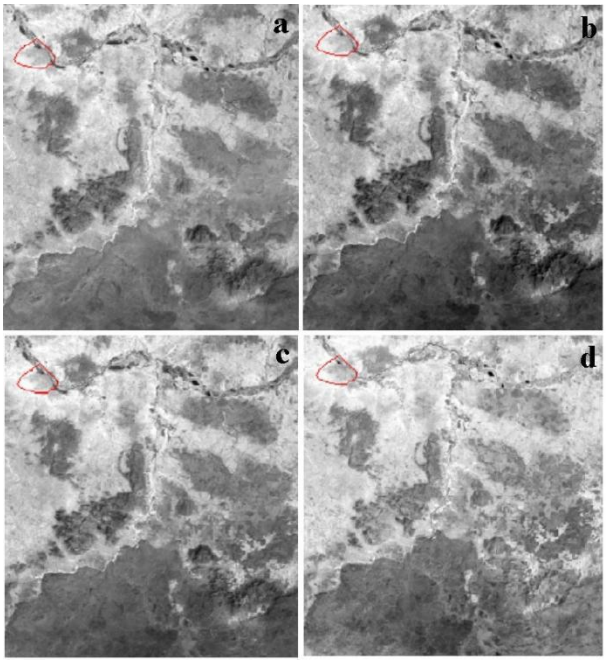

Fig. 2. Multi-spectral bands of Land Sat 8 Operational Land Imager captured on 16th February 2022 Blue (a), Green (b), Red (c), Near Infrared (d).

IV. METHODOLOGY

A. *Image preprocessing*

Because the satellite image was processed in Level-1C format, it was subjected to geometric and radiometric correction but not atmospheric correction [21]. As a result, the "Raster calculator" function in ArcGIS software was used to transform the digital number (raw picture) to top-of-atmosphere reflectance in order to perform an atmospheric correction on satellite images based on (1)

$$P\lambda = \frac{M\rho * DN + A\rho}{Sin(\theta SE)} \quad (1)$$

Where:

Pλ is the top of the atmosphere planetary Reflectance (Adjusted image)

DN is the digital number (specific band of the Land Sat 8)

Mρ is the Multi-band value of band-specific Reflectance

Aρ is the Add Band Value of Band Specific Reflectance

B. *Image Processing*

The images used in this study have many bands, each of which holds a separate set of data. Thus, in order to create a single multi-spectral image file (RGB image), which is helpful for identifying and visualizing bare surfaces, vegetation, and built-up areas, as well as for differentiating features that appear identical [22]. By employing the "Composite band" function in ArcGIS 10.8 software, visible (RGB) and infrared (NIR) were merged (layer stack) to create a multi-spectral false-color composite image (as in Fig. 3).

The area under study accounted for a relatively small part of the multi-spectral picture, which spans over one gigabyte in size. A new image of the research region had been extracted (as seen in Fig. 3) in order to save computational time and storage space for improved image handling and to use only the required portion of the whole data set. The administrative boundary of the study area was used in delineating the region of interest as ArcGIS 10.8's "Clip" tool was used to prepare and clip the images to fit within the desired boundary.

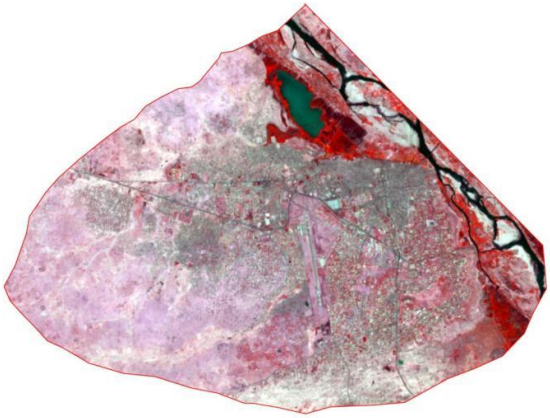

Fig. 3. Study area in false color composite

C. *Deep learning and Machine learning algorithms*

The classification algorithms are explained in this section. Readers who wish to go more into the theoretical underpinnings of the algorithm can consult the reference listed at the conclusion of each explanation.

a) *Artificial Neural Network:* A simulated neural network (SNN) or, more frequently, merely a neural network (NN) are other names for an artificial neural network (ANN). Warren S. McCulloch and Walter Pitts were the ones who initially used the term "Neural

Networks" in the early 1970s. According to [7], ANN is a supervised learning Model which simulates human neural system (a system of interconnected processing elements known as nodes that function similarly to biological neurons). It is a network of artificial neurons that manipulates data using a mathematical model and a mathematical connection technique. The input layer, the output layer, and the hidden layer are the three main layers of a neural network. An ANN has multiple layers, each of which has many neurons, each of which represents a variable from the input layer [23], therefore the simulations work in the same way as biological neural networks in the human brain process information [24]. The input layer is the initial layer of an artificial neural network (ANN) that accepts input data in the form of image pixels. The hidden layers are located in the center of the ANN model. These hidden layers take data from the input and use several kinds of mathematical operations to identify patterns. The hidden layers can be viewed as individual feature detectors, recognizing increasingly complex patterns in data as it travels through the network. The outcome of the middle layer's intensive computations is acquired in the output layer. A neural network's weights, biases, learning rates, and batch sizes are among its essential attributes. The majority of these parameters determine how an ANN performs. In the ANN, a weight (w) is assigned to each node. Feed-forward neural networks generate artificial neurons that send their weight values to the next layer. [25] Multi-layer Perceptron (MLP) is a significant class of feed-forward neural networks [26]. The most popular MLP training method used is the back-propagation algorithm which modifies the weights between neurons in order to reduce errors. An activation function is used to generate the weighted sum of the input values, and a transfer function is used to calculate the weighted sum of the inputs and the bias. [27]. Every class in the classification system via the classification process has a single output node. Furthermore, a high sample size is needed in ANN modeling to prevent overfitting predictions. [28].

b) *Support Vector Machine (SVM):* SVM is a supervised learning technique that enables the accurate classification of data from a set of small training samples [6]. The first SVM algorithm was a linear classifier which was invented by Vapnik in 1963. [29] on the other hand, proposed a method of using the kernel technique on the maximum-margin hyperplane to generate nonlinear classifiers. In order to maximize the margin between various classes, the SVM's main principle is to translate multidimensional data into a higher-dimensional space where an ideal hyperplane may be utilized to divide the original data [30] [31]. SVM uses mathematical manipulation to project the decision boundary back to the original dimensions after adding a dimension to make the data linearly separable [31]. One of the various hyperplanes that can split the data space into two areas is the one that extends the distance between adjacent data points in the input data. Adjacent data points near this hyperplane are support vectors [29]. Consequently, only a subset of training samples is often used as a support vector because not all of them contribute to the creation of the hyperplane [32].

D. Image Classification

a) *Selection of Training samples:* To determine the spectral reflectance pattern or signature of each LULC type, supervised classification requires the use of training samples. [16]. The accuracy of the classification has been shown to be significantly influenced by training data, which establishes the class that each pixel in the image will inherit [17]. The training samples were selected based on the four broad LULC classes in the study area which include Built-up, Vegetation, Water, and Bare soil using Region of Interest (ROI) tools and functions for SVM and ANN classification in ENVI 5.3. The selection was based on stratified random sampling from every LULC feature.

b) *Model training:* Each model was trained using the same set of selected samples. As part of the model training process, the algorithms' ideal hyper-parameters were chosen through hyper-parameter optimization, also known as tuning. Through repeated k-fold cross-validation, hyper-parameter optimization was used to train the models. For SVM, optimization was carried out up to a predetermined number of iterations by randomly selecting every combination of hyperparameters [33]. The training dataset was divided into k equal-sized sets at random; k–1 sample were used for training and one set was kept for validation. Then, in order to lower model variance, the entire process was carried out again using a predetermined set of repeats [34]. As a trade-off between reducing variance, offering a reliable model, and a reasonable processing time, 10-fold cross-validation with five repetitions was used. The SVM was trained with the following optimum parameters: pyramid level-1, pyramid reclassification threshold-0.90, gamma in kernel function-1, kernel type-radial basis function, and penalty parameter-100.

In the case of DL (ANN), a random grid search was used for optimization. In this case, the algorithm trained a model to account for every possible set-up of the grid's hyperparameters and then select the optimal one. Using the labeled training samples, the activation function was utilized to calculate the weights and biases. During the back-propagation phase, a gradient

descent algorithm is utilized to train the network and determine the weights and biases of each layer in order to optimize the weights and minimize the errors. Hidden layer-1, input layer-1, output layer-1, nodes-4, learning rate-0.01, momentum factor-0.5, and sigmoid constant-1 were the optimum parameters. The surface reflectance variables of the bands in the labeled pixel are fed into the model based on these training samples and the architecture. The software used for modelling was ENVI 5.3. All computation was carried out on a Core (TM) i3-5010U CPU 2.10GHz with 8 GB of RAM running on Windows 10, 64-bit.

E. Accuracy Assessment

When determining the quality of information acquired from remotely sensed data, accuracy evaluation is crucial to any classification project given that it correlates the classified image to ground truth data that are collected within the area being studied and is believed to be reliable. [20]. The two hundred (200) ground truth points for the four (4) land use and Land cover classes that were obtained from the field, were used for testing and assessing the accuracy of the classification results obtained by both SVM and ANN algorithms. Confusion matrix technique [35] was utilized to compare the two classification methods (SVM and ANN) following statistical analysis of the ground truth point data and classification outcomes and select the result with the highest accuracy. In order to determine the components of overall accuracy (2), producer (3), and user (4) accuracy, as well as kappa coefficient (5), these standards error matrices were calculated using the same data references for each image, as indicated by several research, including [36] [37] [38].

Overall Accuracy (OA):

$$\mathbf{OA} = \frac{\mathrm{TCP}}{\mathrm{TRP}} * 100 \quad (2)$$

Where:
TCP is the Total number of correctly categorized pixels
TRP is the Total number of Reference Pixels

Producer Accuracy (PA):

$$\boldsymbol{PA} = \frac{\mathrm{SCC}}{\mathrm{CT}} * 100 \quad (3)$$

Where:
SCC is the Correctly identified Samples in the Column
CT is the Column Total

User Accuracy (UA):

$$\boldsymbol{UA} = \frac{\mathrm{SCR}}{\mathrm{RT}} * 100 \quad (4)$$

Where:
SCR is the correctly identified Samples in the Row
RT is Row Total

Kappa coefficient (KC):

$$\mathbf{KC} = \frac{(\boldsymbol{TS} * \boldsymbol{TCS}) - \Sigma\,(\mathbf{CT} * \mathbf{RT})}{\boldsymbol{TS}^2 - \Sigma\,(\mathbf{CT} - \mathbf{RT})} \quad (5)$$

Where:
TS is the Total sample
TCS is the Total number of the correctly classified sample
CT is the Column Total
RT is the Row Total

The total number of successful classifications across all samples (ground truth points) in the classified picture is known as overall accuracy (OA). It is computed by adding up all of the values that were properly identified and dividing that amount by all of the values in the confusion matrix. [36]. on the other hand, the kappa coefficient (KC) is a discrete multivariate approach for determining the level of agreement or accuracy [39]. The KC is a metric for estimating the actual degree of agreement between an automated classifier and reference data. Its value falls between −1 and 1 [40]. but, it usually lies in the range of 0 to 1 [41]. The algorithm's likelihood of satisfying the minimum accuracy requirement for the classified images was determined by comparing its overall accuracy with more than 85% [42] and Kappa value above 0.75 [43, 11]

F. Area Estimation

The simulation tool used for area estimation was ArcGIS 10.8 and Microsoft Excel software. The first step in Area estimation of the mapped classes involves raster to vector conversion in ArcGIS 10.8 software, as follows:

Arc tool Box:

- Conversion Tools
- From Raster
- Raster to Polygon
- Input Raster (include class in the attribute table of the raster data)
- Select the class created in the raster
- Ok.

The vector data (polygon) was dissolved in the second stage. The procedures that were followed were as follows:

Geo-processing

- Dissolve
- Input feature class (Add the vector file to be dissolved)
- dissolve field (select the field to be dissolved)
- Ok

The last stage was Computing the Area covered by LULC classes. The procedures are as follows:

Open the attribute table of the unified vector (shape file)

- Add another field (Area)
- right-click on the field
- Calculate Geometry
- Yes
- Change the unit to Kilometers square
- Ok

Exporting the files to Microsoft Excel

- Export the attribute table
- Table Options
- Export
- the file extension was Changed to dBASE Table
- Save
- OK

After exporting, Microsoft Excel was opened. First, a pivot table for the two images was created, and then the relevant statistics were used to ascertain the variations in land use/cover.

V. RESULT AND DISCUSION

A. *Land use and Land Cover Classification of the study area produced by ANN*

The Land Use and Land Cover map generated by ANN shows that bare surface covered the largest portion of total area representing 59.15 km² (52.46%), followed by vegetation 5.88 km² (5.21%), while built-up area occupied 44.5km² (39.48%) of the total land area. water is the least covering an area of 3.21 km² (2.85%) (Fig. 4a and Table 2). ANN was able learn and capture the intricate patterns in satellite imagery. ANN was also able to correctly classify the majority of pixels that correspond to classes. This is in line with [13] who observed that for the Land cover classification using Sentinel 2A in the city of Soran, Kurdistan Region, Iran, the majority of pixels were accurately identified by ANN. The results, however showed that misclassification of LULC feature were occurred. Some portions of the subset; built-up, water, and vegetation are incorrectly classified as bare surface. This shows that ANN overestimated bare surface and underestimated built-up, water, and vegetation. This finding is consistent with that of [10] who identified issues with artificial neural network's misclassification in a crop type mapping using Sentinel-1 and Sentinel-2 images in a semi-arid region of Central Morocco.

B. *Land use and Land Cover Classification of the study area produced by SVM*

Fig. 4b depicts the multi-temporal LULC visualizations created using SVM, which are divided into four main classes: vegetation, bare soil, built-up areas, and water bodies. TABLE 2 revealed that Built-up covered 58.556 km² (51.94%). Water bodies covered 2.683km² (2.38%), while bare surface occupied 36.701km² (32.55%). On the other hand, vegetation occupied 14.8 km² representing 13.13% of the study area. . SVM was able to find an optimal hyperplane, which leads to better generalization and robust classification performance. As a result, SVM generated visually pleasing maps with few specks and coherent classes that accurately represented the area. This means that SVM has properly defined all of the LULC characteristics. This is consistent with the findings of [11] who stated that SVM fairly delineated LULC features in a land cover and land use classification of a volcanic island using Landsat 8 OLI image in the Aleutian Arc, USA, and with the findings of [9] who reported that utilizing Sentinel-2 images for Land Use Land Cover Classification in South Central Sweden, SVM maintained a high identification rate while properly delineating a boreal landscape. Thus, it can be concluded that the SVM was highly effective in computing and had a significant recognition rate

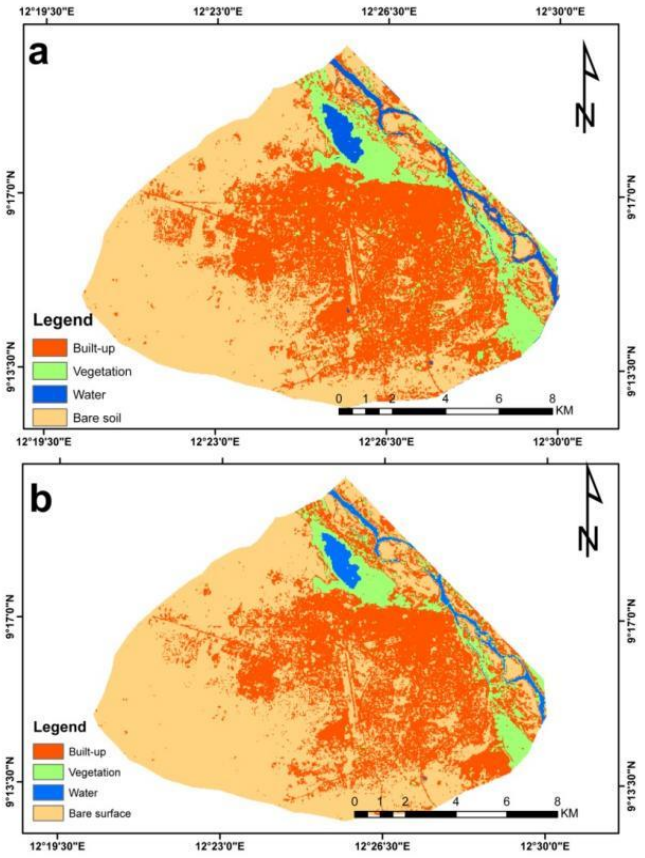

Fig. 4. Final classified maps of the area of study for (a) Artificial Neural Networks; (b) Support Vector Machines

C. *Classifiers' comparison and Variation in classification results generated by ANN and SVM*

All classification methods indicated bare surface as the most dominant LULC class in the region, according to the classification maps created by SVM and ANN classifiers shown in Fig. 4 and TABLE 2. Water was also found to be the land cover feature with the least area of coverage using all of the methodologies. Nevertheless, some differences between the classifications of SVM and ANN models were noticed (TABLE 2). In fact, inconsistencies in classifications with all classes were observed. The area for every LULC category in relation to the study area's overall land coverage for every classifier is displayed in TABLE 2. Based on the results of SVM and ANN, the proportion of the entire area that was bare soil ranged from 36.701 km² (32.55%) to 59.15 km² (52.46%), Vegetation varied from 5.88km² (5.21%) by ANN to 14.8km² (13.13%) by SVM, Water also varied from 3.21km² (2.85%) by ANN to 2.683km2 (2.38%) by SVM. On the other hand, the area covered by built-up varied from 44.5Km2 (39.48%) by ANN to 58.556Km2 (51.94%) by SVM.

TABLE 2. Variation in Lulc Statistics Generated by the two Algorithms

Classes	ANN		SVM	
	Area (Km2)	%	Area (Km2)	%
Built-up	44.5	39.48	58.556	51.94
Vegetation	5.88	5.21	14.8	13.13
Water	3.21	2.85	2.683	2.38
Bare soil	59.15	52.46	36.701	32.55
Total	112.74	100	112.74	100

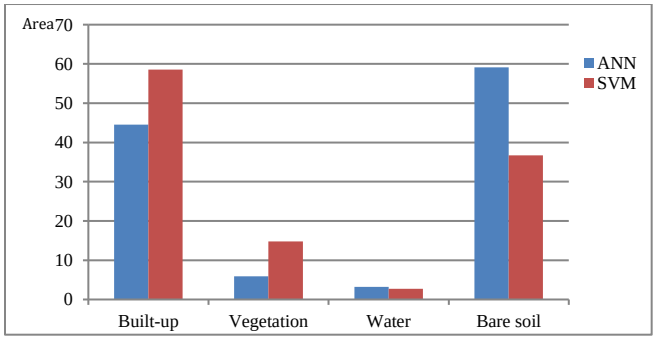

Fig. 5. Difference in area estimation for every LULC classes as a consequence of classifying images using the two tested methods (Artificial Neural Network (ANN); Support Vector Machine (SVM))

The highest coverage of water bodies is provided by the ANN classifier, whereas the largest coverage of vegetation is provided by the SVM (Fig. 5). This shows a disparity in the LULC classifications generated by the two classifiers, such as SVM and ANN, perhaps as a result of how differently each learns. This agrees with the results of [14] who claimed that there was variation in LULC classification using Landsat 8 OLI image generated by SVM and ANN in research conducted in the River Ganga from Rajmahal to Farakka barrage, India. The variations in model parameter optimization, methods, and algorithmic accuracy are the reasons for the differing results in the area under LULC classes of the two classifiers.

D. Accuracy Assessment of the classification results

A classification's accuracy varies depending on the procedures, techniques, period, and location. [3] [44] [45]. Numerous studies found that the accuracy of the LULC classification varied from minimal to significant when alternative classifiers were used. [12] [13]. A little variance exists between the classifiers' outputs in the current instance, based on the study's accuracy evaluation. Space and the quantity of the training sample affect the accuracy of a LULC classification in addition to the classifier. Confusion matrices of each classification method were generated to analyze classes' separation performance. Each classifier was assessed with evaluation metrics (including Overall accuracy, User and Producer Accuracy, and Kappa Coefficient). The findings revealed that the SVM technique has the best overall accuracy of 95.5% and Kappa Coefficient (0.94). This result agrees with the result obtained by [12] who stated that SVM attained a minimal degree of accuracy, attaining 96.58% overall accuracy and a 0.9591 Kappa value. and also recorded the highest as compared with RF and ANN in LULC classification of Sentinel-2 medium resolution optical satellite image focusing on inundated regions in flat areas in the South of Hungary. This finding is above the current study's results. On the other hand, ANN achieved a 0.86 Kappa Coefficient and an overall accuracy percentage of 89.5%. Prior research on LULC classification with ANN classifiers revealed 90% and 0.86 accuracy levels for OA and KC, respectively [13] which is almost close to the findings of the current study. The Accuracy assessment for each algorithm and LULC classes derived from the confusion matrix are provided in TABLE 3. The impact of the training samples on the outcome was significant. According to [42] a minimum level of accuracy approximating 85% is adequate for the classification of LULC features. On the other hand, [43] stipulated that a Kappa value above 0.75 is adequate for the classification of LULC features. This means that the 95.5% overall accuracy of the classification result generated by SVM was excellent and also the Kappa Value of 0.94 signifies a significant and nearly perfect kappa coefficient, implying that SVM attained the minimum level of accuracy and produced the best outcome when compared to ANN.

The user and producer accuracies however varied between the LULC classes and classifiers as shown in TABLE 3. Both Producer and User accuracy was highest in water (100%) using the SVM classifier, while the low user (84.5%) was obtained for bare soil by ANN. The highest user and producer accuracies were achieved by SVM for the individual classes (TABLE 3).

TABLE 3. Accuracy Assessment of the Classification Algorithms Derived from the Confusion Matrix

Algorithms	**Classes**	**User Accuracy**	**Producer Accuracy**
SVM	Built-up	94%	92.2%
OA=95.5%	Vegetation	94%	95.9%
KC=0.94	Water	100%	100%
	Bare soil	94%	94%
ANN	Built-up	92%	88.5%
OA=89.5%	Vegetation	82%	83.7%
KC=0.86	Water	100%	98.04%
	Bare soil	84%	87.5%

The higher producer accuracy obtained in the LULC features (water and Built-up) could be due to their very low spectral confusion. For the vegetation, the ANN classification approach exhibits comparatively substantial erroneous The resolution of the land-sat data may be the primary cause of this, because of mixed pixels in the vegetation. The highest user and producer accuracy in bare soil produced by SVM is probably due to the

higher spectral quality of Land sat 8 OLI data utilized and based on the SVM's relatively small number of complex decision boundaries. The aforementioned claim is demonstrated by [9] who confirmed that the ability of SVM to produce the highest accuracy for bare soil was based on a fairly limited number of complex decision boundaries.

Both methods were able to handle the high-dimensional feature spaces (that is, the Land Sat image), making them versatile choice for satellite image classification tasks. however, the training samples significantly influenced the final result. The highest accuracy achieved by SVM is attributed to the classifier's capacity to produce meaningful results with minimal training samples [6] as it's less prone to overfitting. Whereas, the low performance of ANN could be attributed to the classifier's inability to produce an accurate result with minimum training samples, this is because ANN is prone to overfitting and requires a large training sample to accurately classify data [28]. While SVM performance can be affected by the choice of kernel function and hyperparameters, ANN requires a large amount of training data and computational resources for training.

VI. CONCLUSION

The SVM approach yielded results with the best overall classification accuracy. Therefore, it can be concluded that maps generated by SVM are the best classifiers for LULC classification in the study area. All methods of classification indicated the bare soil as the LULC feature with the largest area and water as the land cover feature with the smallest area of coverage. However, some distinctions between LULC maps generated by the ANN and SVM model classifications were found. The study revealed that the highest accuracy achieved by SVM is attributed to the classifier's capacity to produce meaningful results with minimal training samples. Moreover, variations in model parameter optimization, approaches, and algorithm accuracy all contribute to variance in the area within the LULC classes of the two classifiers. This study contributed to the understanding of existing classification methods, to choose which of their performances is most suitable for study. Moreover, a number of researches revealed that model setup and geographical distribution affect LULC classification accuracy. Therefore, it is recommended that future researches focus on exploring hybrid approaches for improved classification accuracy to overcome the limitations of the models.

VII. ACKNOWLEDGMENT

Sincere gratitude is extended to the United States Geological Survey (USGS) for providing Land sat imagery for the research area. We appreciate the Administrative Boundary Shape File being provided by GRID 3 Nigeria. We are also grateful for the Global Positioning System (GPS) device provided by the Zonal Advanced Space Technology Application Laboratory (ZASTAL), Kano.

REFERENCES

[1] Delalay, M., Tiwari, V., Ziegler, A.D., Gopal, V., & Passy, P., "Land-use and land-cover classification using Sentinel-2 data and machine-learning algorithms, operational method and its implementation for a mountainous area of Nepal," Journal of Applied Remote Sensing, vol. 13, no. 1, p. 247–259, 2019.

[2] Yan, J., Wang, L., Song, W., Chen, Y., Chen, X., & Deng, Z., "A time-series classification approach based on change detection for rapid land cover mapping," Journal of Photogrammetry and Remote Sensing, vol. 158, pp. 249-262, 2019.

[3] Camargo, F.F.; Sano, E.E.; Almeida, C.M.; Mura, J.C.; Almeida, T. A, "Comparative assessment of machine-learning techniques for land use and land cover classification of the Brazilian tropical savanna using ALOS-2/PALSAR-2 polarimetric images," Remote Sensing, vol. 11, no. 1600, 2019.

[4] Nogueira, K., Otávio, A.B., Jefferson P.A. & Santos, D., "Towards better exploiting Convolution neural networks for remote sensing scene classification," Pattern Recognition, vol. 61, pp. 539-556, 2017.

[5] k. Rendy, "Google Earth Engine Machine Learning for Land Cover Classification with Code," Google Earth Engine, [Online]. Available: https://www.analyticsvidhya.com/blog/2021/04/google-earth-engine-machine-learning-for-land-cover-classification-with-code/. [Accessed 2 September 2021].

[6] Birzhandi, P., Kim, K., & Youn, H., " Reduction of training data for support vector machine: a survey," Soft Computing, vol. 26, pp. 1-14, 2022.

[7] Shih, H., Stow, D. A., & Tsai, Y. H., "Guidance on and comparison of machine learning classifiers for Landsat-based land cover and land use mapping," International Journal of Remote Sensing, vol. 40, no. 4, pp. 1248-1274, 2019.

[8] A. Gupta, "Introduction to Deep Learning: Part 1," 2018. [Online]. Available: www.aiche.org/sites/default/files/cep/20180622.pdf. [Accessed 3 July 2023].

[9] A. Abdi, "Land cover and land use classification performance of machine learning algorithms in a boreal landscape using Sentinel-2 data," GIScience & Remote Sensing, vol. 51, no. 1, pp. 1-20, 2020.

[10] Moumni, A., & Lahrouni, A., "Machine Learning-Based Classification for Crop-Type Mapping Using the Fusion of High-ResolutionSatellite Imagery in a Semiarid Area," Hindawi Scientifica, vol. 2021, 2021.

[11] Kadavi, P.R. & Lee, C.W., "Land cover classification analysis of volcanic island in an Aleutian arc using an artificial neural network (ANN) and a support vector machine (SVM) from Landsat imagery," Geosciences Journal, vol. 22, pp. 653-665, 2018.

[12] Leeuwen, B. V., Tobak, Z., & Kovacs, F., "Machine learning techniques for land use/land cover classification of medium resolution optical satellite imagery focusing on temporary inundated areas," Journal of Environmental Geography, vol. 13, no. 12, pp. 43-52, 2020.

[13] R. Hamad, "An assessment of artificial neural networks, support vector machines and decision trees for land cover classification using sentinel-2A data," Applied Ecology and Environmental Sciences,, vol. 8, no. 6, p. 459–464, 2020.

[14] Talukdar, S., Singha, P., Mahato, S., Fahad, S., Pal, S., Liou, Y.A., & Rahman, A., "Land Use Land Cover Classification by Machine Learning Classifiers for Satellite Observations: A Review," Remote Sensing,, vol. 12, no. 7, p. 1135, 2020.

[15] Faisal, A. K., Yue, W., Abdullahi, G. A., Hamed, R., & Akram, A. N. A., "Analyzing urban growth and land cover change scenario in Lagos, Nigeria using multi-temporal remote sensing data and GIS to mitigate flooding," Geomatics, Natural Hazards, and Risk, vol. 12, no. 1, pp. 631-652, 2021.

[16] Muhammad, B. U., Ismaila, A.B., & Aliyu. I., "An Analysis of Urban Growth Pattern in Yola-North Local Government Area, Adamawa State, Nigeria," Journal of Environmental and Social Sciences, vol. 24, no. 3, 2018.

[17] Petitjean, F., Inglada, J., & Gancarski, P., "Satellite Image Time Series Analysis Under Time Warping, IEEE Transactions on Geosciences and Remote Sensing," vol. 50, no. 8, pp. 3081-3095, 2012.

[18] Yu, X., Lu, D., Jiang, X., Li, G., Chen, Y., Li, D., & Chen, E., "Examining the Roles of Spectral, Spatial, and Topographic Features in Improving Land-Cover and Forest Classifications in a Subtropical Region," Remote Sensing, vol. 12, no. 18, p. 2907, 2020.

[19] T. Joseph, "Understanding Artificial Neural Networks, Examining the fundamentals of deep learning models and neural networks.," Towards data science., 2020. [Online]. Available: towardsdatascience.com/understanding-artificial-neural-networks-3fc3cbcd397d. [Accessed 16 October 2023].

[20] A. Anad, "Accuracy Assessment," www.researchgate.net/publication/324943246, 2017.

[21] Drusch, M., U. Del Bello, S. Carlier, O. Colin, V. Fernandez, F. Gascon, B. & Hoersch E., "Sentinel-2: ESA's Optical High-Resolution Mission for GMES Operational Services," Remote Sensing of Environment, vol. 20, pp. 25-36, 2012.

[22] Ettehadi, O., Paria, S. K., Elif S., & Ugur, A., "Separating Built-Up Areas from Bare Land in Mediterranean Cities Using Sentinel-2A Imagery," Remote Sensing, vol. 3, no. 345, p. 11, 2019.

[23] Kesikoglu, M.H., Atasever, U.H., Dadaser-Celik, F., & Ozkan, C, "Performance of ANN, SVM and MLH techniques for land use/cover change detection at Sultan Marshes wetland, Turkey.," Water Science Technology,, vol. 80, no. 3, pp. 466-477, 2019.

[24] Liu, C., Zhang, L., Davis, C.J., Solomon, D. S., Brann, T. B., Caldwell, L.E, "Comparison of neural networks and statistical methods in classification of ecological habitats using FIA data.," Forest Science, vol. 49, pp. 619-631, 2003.

[25] Bebis, G., & Georgiopoulos, M., "Feed-forward Neural Networks," IEEE Potentials, vol. 13, no. 4, pp. 27-31, 1994.

[26] S. Haykin, Neural Networks, and Learning Machines, Upper Saddle River-3: Pearson, 2009.

[27] Saritas M. M., & Yasar, A., "Performance Analysis of ANN and Naive Bayes Classification Algorithm for Data Classification," International Journal of Intelligent System and Applications Engineering, vol. 7, no. 2, pp. 88-91, 2019.

[28] Ngoc-Thuy Vu, Khac-Uan Do,, "Prediction of Ammonium Removal by Biochar Produced From Agricultural Wastes Using Artificial Neural Networks: Prospects and Bottlenecks," Soft Computing Techniques in Solid Waste and Wastewater Management, Elsevier, pp. 455-467, 2021.

[29] Boser, B. E., Guyon, I. M., & Vapnik, V. N., "A training algorithm for optimal margin classifiers," in Theory, Proceedings of the 5th Annual Workshop on Computational Learning., Pittsburgh, 1992.

[30] V. Vapnik, Statistical learning theory, New York: John Wiley., 1998.

[31] R. Pupale, "Support Vector Machines (SVM): An Overview.," Towards data science, 2018. [Online]. Available: towardsdatascience.com/https-medium-com-pupalerushikesh-svmf4b42800e989. [Accessed 20 June 2023].

[32] Tso, B., & Mather, P., Classification Methods for Remotely Sensed Data., Boca Raton, FL: CRC Press, Taylor & Francis Group. 376, 2009.

[33] Bergstra, J., and Y. Bengio, "Random Search for Hyper-parameter Optimization.," Journal of Machine Learning Research , vol. 13, no. 2, pp. 281-305, 2012.

[34] J. Kim, "Estimating Classification Error Rate: Repeated Cross-validation, Repeated Hold-out and Bootstrap," Computational Statistics & Data Analysis, vol. 53, no. 11, pp. 3735-3745, 2009.

[35] Congalton, R.G., & Green, K., "Assessing the Accuracy of Remotely Sensed Data: Principles and Practices, Third Edition (3rded.).," CRCPress, 2019.

[36] Aljenaid, S.S., Ghadeer, R. Kadhem G.R., Manaf F. AlKhuzaei, M.F., Jobair B., & Alam, J.B., "Detecting and Assessing the Spatio-Temporal Land Use Land Cover Changes of Bahrain Island during 1986–2020 Using Remote Sensing and GIS," Earth Systems and Environment , 2021.

[37] Sophia, R., & Julius, N, "Accuracy Assessment of Land Use Land Cover Classification Using Remote Sensing and GIS," International Journal of Geosciences., vol. 8, pp. 611-622, 2017.

[38] Adeyemi, A.A., & Oyeleye, H.A, "Evaluation of land-use and land-cover changes cum forest degradation in Shasha forest reserve, Osun state, Nigeria using remote sensing," Tanzania Journal of Forestry and Nature Conservation, vol. 90, no. 2, pp. 27-40, 2021.

[39] Koc, D., Ikiel, C., Atalay, A., & Ustaoglu, B, "Land use and land cover (LULC) classification using spot-5 image in the Adapazari plain and its surroundings, Turkey.," Online Journal of Science and Technology,, vol. 2, pp. 37-42, 2012.

[40] Tang, W., Hu, J., Zhang, H., Wu, P., & He, Hu, "Kappa coefficient: a popular measure of rater agreement," Shanghai archives of psychiatry, vol. 27, pp. 62-70, 2015.

[41] Zanotta, D.C., Zortea, M., & Ferreira, M. P, "A supervised approach for simultaneous segmentation and classification of remote sensing images," ISPRS Journal of Photogrammetry and Remote Sensing, vol. 142, pp. 162-173, 2018.

[42] Anderson, J.R., Hardy, E.E., Roach, J.T., & Witmer, R.E., "A land use and land cover classification system for use with remote sensor data.," United States Government Printing Office, Washington, D.C., 1976.

[43] Fleiss, J.L, Levin, B., & Paik, M.C., The measurement of interrater agreement, S. S. W. Walter A. Stewart, Ed., Wiley online library, 2003, p. 598–626.

[44] Noi, P.T. & Kappas, M., "Comparison of Random Forest, k-Nearest Neighbor, and Support Vector Machine Classifiers for Land Cover Classification Using Sentinel-2 Imagery," Sensors, vol. 18, no. 18, 2018.

[45] Rodriguez-Galiano, V.F. & Chica-Rivas, M, "Evaluation of different machine learning methods for land cover mapping of a Mediterranean area using multi-seasonal Landsat images and Digital Terrain Models," International Journal on Digital Earth, vol. 7, pp. 492-509, 2014.